Inorg. Chem. **2005**, *44*, 8749–8755

Architectural Isomerism in the Three-Dimensional Polymeric Spin Crossover System $\{Fe(pmd)_2[Ag(CN)_2]_2\}$: Synthesis, Structure, Magnetic Properties, and Calorimetric Studies

Ana Galet,[‡] M. Carmen Muñoz,[‡] Ana B. Gaspar,[†] and José A. Real*[,†]

Institut de Ciència Molecular/Departament de Química Inorgánica, Universitat de València, Doctor Moliner 50, 46100 Burjassot, Spain, and Departament de Física Aplicada, Universitat Politècnica de València, Camino de Vera s/n, 46071 Valencia, Spain

Received June 6, 2005

Two coordination polymers formulated $\{Fe(pmd)_2[Ag(CN)_2]_2\}$ (pmd = pyrimidine) have been synthesized and characterized. Both polymers, considered to be architectural isomers, display different crystal structures and magnetic properties. Isomer **1** crystallizes in the monoclinic *C*2/*c* space group with $a = 6.9750(8)$ Å, $b = 16.1700(9)$ Å, $c = 14.2020(8)$ Å, $\beta = 97.954(2)°$, $V = 1586.37(14)$ Å^3, and $Z = 4$. The crystal structure of isomer **2** has been studied at 250 and 150 K. At both temperatures, **2** displays the orthorhombic *Pccn* space group with $a = 15.7700(2)$ [14.8950(2)] Å, $b = 8.2980(4)$ [8.1580(4)] Å, $c = 13.4180(6)$ [13.3480(5)] Å, $V = 1755.87(14)$ [1621.96(10)] Å^3, and $Z = 4$ for 250 [150] K. The iron(II) ions define distorted octahedral $[FeN_6]$ chromophores in both isomers. The equatorial positions are occupied by four $[Ag(CN)_2]^-$ bridging ligands, which connect the defining layers of two iron(II) ions. Isomer **1** has two crystallographically distinct $[Ag(CN)_2]^-$ groups; one is essentially linear, while the other is severely distorted [C(5)–Ag(2)–C(5^i)] = 138.8(5)°. This fact facilitates the parallel interpenetration of two layers, which in addition show short Ag(1)····Ag(2) interactions (distance Ag(1)····Ag(2) = 2.9972(10) Å). Isomer **2** shows only one type of Ag atom, which is slightly bent [C–Ag–C = 161.54(12)°], and as a consequence, the layers defined are not interpenetrated. In both cases, the axial positions are occupied by the pmd ligands which interact with the Ag atoms of adjacent layers defining a 3D coordination polymer. Compound **1** is high spin in the whole range of temperatures, while **2** undergoes a cooperative high-spin ↔ low-spin effect centered at ca. 184 K with a hysteresis loop ca. 5 K wide. The experimental enthalpy and entropy variations were 11.5 ± 0.4 kJ mol^{-1} and 64 ± 3 J K^{-1} mol^{-1}. Consistency between the experimental thermodynamic data and the magnetic data was checked in the frame of regular solution theory.

Introduction

The construction of crystalline coordination polymers displaying physical and chemical properties ranging from magnetism, conductivity, or optical properties to porous functions such as sorption−desorption, exchange, separation, and catalysis is an important topic in current chemistry.[1] A singular aspect of this topic concerns the combination of two or more of these properties in the same solid to investigate possible interplay and synergy between them. This has created important expectations in the search for new properties and multifunctionality.[2] Particularly well adapted to these goals are coordination polymers made up of switchable building blocks, as cooperativity, stemming from interactions among them resulting from the change of state, can confer bistability to the framework and, hence, sensory and memory functions to the solid. Spin crossover building blocks based on $3d^4$−$3d^7$ metal ions are particularly well adapted to this strategy, as their labile electronic configurations may be switched reversibly between the high-spin (HS) and the low-spin (LS) states involving magnetic, optical, and structural changes stimulated by the action of temperature, pressure, or light.[3]

* To whom correspondence should be addressed. E-mail: jose.a.real@uv.es.
† Universitat de València.
‡ Universitat Politècnica de València.

(1) (a) Lehn, J. M. *Science* **2002**, *295*, 2400. (b) Hollingsworth, M. D. *Science* **2002**, *295*, 2410. (c) Kitagawa, S.; Kitaura, R.; Noro, S.-I. *Angew. Chem., Int. Ed.* **2004**, *43*, 2334.

(2) (a) Langley, P. J.; Hulliger, J. *Chem. Soc. Rev.* **1999**, *28*, 279. (b) Beauvais, L. G.; Long, J. R. *J. Am. Chem. Soc.* **2002**, *124*, 12098.

10.1021/ic0509074 CCC: $30.25
Published on Web 10/25/2005

During the last five years we have systematically been investigating new iron(II) spin crossover compounds with polymeric structures based on cyanometalate complexes as bridging ligands. In this respect, Hofmann-like clathrate compounds[4] containing iron(II) ions have led to the development of a number of two-dimensional (2D) and three-dimensional (3D) polymeric singular coordination (SCO) networks, such as $\{Fe(L)_x[M^{II}(CN)_4]\}\cdot nH_2O$ [L = pyridine, $x = 2$, $n = 0$;[5] L = pyrazine, $x = 1$, $n = 2-4$;[6] M^{II} = Ni, Pd, and Pt], which display abrupt thermal and pressure induced transitions and hysteresis at temperatures close to room temperature.[7] The water content affects dramatically the completeness and the critical temperature of the transition in these porous polymers. However, the transition is complete for the monohydrate and anhydrous derivatives and room temperature (ca. 298 K) is included in the large thermal hysteresis loop exhibited for the Pd and Pt derivatives. Interestingly, it has been shown that the LS state can be reversibly switched to the HS state using a one-shot laser pulse in the complex $\{Fe(C_4H_4N_2)[Pt(CN)_4]\}$ at room temperature.[8]

Formal replacement of the $[M^{II}(CN)_4]^{2-}$ anions by $[M^{I}(CN)_2]^{-}$ groups (M^{I} = Cu, Ag, and Au), with *trans*-bispyridylethylene, 4,4′-bipyridine, 3-cyanopyridine, or pyrimidine (pmd) as ligands, has resulted in new 2D and double or triple interpenetrated 3D SCO polymers.[9] Such compounds combine their cooperative SCO properties (magnetic, chromatic, and structural) with different chemical properties such as specific host−guest interactions as in $\{Fe(pyrazine)[M^{II}(CN)_4]\}\cdot$solvent,[10] crystalline-state reactions with allosteric effects as in $\{Fe(pmd)(H_2O)[M^{I}(CN)_2]_2\}\cdot H_2O$ (M^{I} = Ag and Au),[9c] or SCO tuned metallophilicity as in $\{Fe(3\text{-cyanopyridine})[Ag(CN)_2]_2\}\cdot {}^1/_3H_2O$.[9d] More recently the unprecedented 3D polymer $\{Fe(pmd)[Ag_2(CN)_3][Ag(CN)_2]\}$, which displays a thermal and light induced spin transition and spin-dependent ligand unsupported argentophilic interactions, has been reported.[11] In summary, these materials offer the opportunity to investigate the interplay between different switchable molecular and/or supramolecular components and the collective properties that may arise from the synergy between the individual component properties. In this respect, supramolecular or architectural isomerism in coordination polymers is an issue that has received increasing interest in recent years for fundamental and applied reasons.[12] Architectural isomorphism may be particularly meaningful in the realm of polymeric SCO materials, as the building blocks are strongly sensitive probes to detect superstructural diversity. A first example of architectural isomerism in the SCO polymer system $\{Fe(3\text{-cyanopyridine})[Au(CN)_2]_2\}\cdot nH_2O$ was recently communicated.[13]

As a continuation of this systematic research of polymeric systems exhibiting cooperative thermal, pressure, and light induced SCO phenomena, here we report the synthesis, crystal structures, and magnetic and calorimetric studies of the system $\{Fe(pmd)_2[Ag(CN)_2]_2\}$, which affords an interesting example of architectural isomerism based on the distortion of the usually rigid $[Ag(CN)_2]^-$ group.

Experimental Section

Materials. $Fe(BF_4)_2\cdot 6H_2O$, pmd, and $K[Ag(CN)_2]$ were purchased from commercial sources and used as received.

Preparation of Polymorphs A (1) and B (2). **1** and **2** were synthesized in the same reaction from the slow diffusion of two aqueous solutions. One contained a mixture of stoichiometric amounts of $Fe(BF_4)_2\cdot 6H_2O$ (0.185 mmol, 2 mL) and pmd (0.374 mmol, 2 mL) in one side of an H-shaped vessel. The other side contained a solution of $K[Ag(CN)_2]$ (0.374 mmol, 2 mL). Pale-yellow (**1**) and orange-yellow (**2**) prismatic crystals were formed two weeks later and separated using a binocular lens. All the manipulations were performed under an argon atmosphere at 303 K. Yield: ca. 30% (**1**) and 20% (**2**). Anal. Calcd for $C_{12}H_8N_8Ag_2Fe$ (**1**): C, 26.90; H, 1.50; N, 20.91. Found: C, 26.7; H, 1.6; N, 21.0. Anal. Calcd for $C_{12}H_8N_8Ag_2Fe$ (**2**): C, 26.90; H, 1.50; N, 20.91. Found: C, 26.9; H, 1.5; N, 20.8.

Magnetic Measurements. The variable temperature magnetic susceptibility measurements were carried out on samples constituted of small single crystals (20−30 mg) using a Quantum Design MPMS2 SQUID susceptometer equipped with a 5.5 T magnet and operating at 1 T and 1.8−300 K. The susceptometer was calibrated with $(NH_4)_2Mn(SO_4)_2\cdot 12H_2O$. Experimental susceptibilities were corrected for the diamagnetism of the constituent atoms by the use of Pascal's constants.

X-ray Crystallography. Diffraction data on prismatic crystals was collected at 293 K for **1** and at 250 and 150 K for **2** with a Nonius Kappa-CCD single-crystal diffractometer using Mo Kα radiation ($\lambda = 0.71073$ Å). A multiscan absorption correction was performed but not applied. The absorption correction was found to have no significant effect on the refinement results. The structures were solved by direct methods using SHELXS-97 and refined by

(3) (a) Gütlich, P., Goodwin, H. A., Eds. *Spin Crossover in Transition Metal Compounds*; Topics in Current Chemistry; Springer: New York, 2004; Vols. 233−235. (b) Real, J. A.; Gaspar, A. B.; Niel, V.; Muñoz, M. C. *Coord. Chem. Rev.* **2003**, *235*, 121. (c) Gütlich, P.; Hauser, A.; Spiering H. *Angew. Chem., Int. Ed. Engl.* **1994**, *33*, 2024. (d) König, E. *Struct. Bonding (Berlin)* **1991**, *76*, 51. (e) König, E.; Ritter, G.; Kulshreshtha, S. K. *Chem. Rev.* **1985**, *85*, 219. (f) Gütlich, P. *Struct. Bonding (Berlin)* **1981**, *44*, 83. (g) Goodwin, H. A. *Coord. Chem. Rev.* **1976**, *18*, 293.

(4) Iwamoto, T. In *Inclusion Compounds*; Atwood, J. L., Davies, J. E. D., MacNicol, D. D., Eds.; Oxford University Press: London, U.K., 1991; Vol. 5, p 177.

(5) Kitazawa, T.; Gomi, Y.; Takahashi, M.; Takeda, M.; Enemoto, A.; Miyazaki, T.; Enoki, T. *J. Mater. Chem.* **1996**, *6*, 119.

(6) Niel, V.; Martinez-Agudo, J. M.; Muñoz, M. C.; Gaspar, A. B.; Real, J. A. *Inorg. Chem.* **2001**, *40*, 3838.

(7) Molnár, G.; Niel, V.; Real, J. A.; Dubrovinsky, L.; Bousseksou, A.; McGarvey, J. J. *J. Phys. Chem. B* **2003**, *107*, 3149.

(8) Bonhommeau, S.; Molnár, G.; Galet, A.; Zwick, A.; Real, J. A.; McGarvey, J. J.; Bousseksou, A. *Angew. Chem., Int. Ed.* **2005**, *44*, 4069.

(9) (a) Niel, V.; Muñoz, M. C.; Gaspar, A. B.; Galet, A.; Levchenko, G.; Real, J. A. *Chem.—Eur. J.* **2002**, *8*, 2446. (b) Niel, V.; Galet, A.; Gaspar, A. B.; Muñoz, M. C.; Real, J. A. *Chem. Commun.* **2003**, 1248. (c) Niel, V.; Thompson, A. L.; Muñoz, M. C.; Galet, A.; Goeta, A. E.; Real, J. A. *Angew. Chem., Int. Ed.* **2003**, *42*, 3759. (d) Galet, A.; Niel, V.; Muñoz, M. C.; Real, J. A. *J. Am. Chem. Soc.* **2003**, *125*, 14224.

(10) Niel, V. Ph.D. Thesis, Universitat de València, Burjassot, Spain, 2002.

(11) Niel, V.; Thompson, A. L.; Goeta, A. E.; Enachescu, C.; Hauser, A.; Galet, A.; Muñoz, M. C.; Real, J. A. *Chem.—Eur. J.* **2005**, *11*, 2047.

(12) (a) Swift, J. A.; Pivovar, A. M.; Reynolds, A. M.; Ward, M. D. *J. Am. Chem. Soc.* **1998**, *120*, 5887. (b) Moulton, B.; Zaworotko, M. J. *Chem. Rev.* **2001**, *101*, 1629. (c) Hennigar, T. L.; MacQuarrie, D. C.; Losier, P.; Rogers, R. D.; Zaworotko, M. J. *Angew. Chem., Int. Ed. Engl.* **1997**, *36*, 972.

(13) Galet, A.; Muñoz, M. C.; Martínez, V.; Real, J. A. *Chem. Commun.* **2004**, 2268.

Table 1. Crystal Data for **1** and **2**

	1	**2** (250 K)	**2** (150 K)
empirical formula	$C_{12}H_8N_8Ag_2Fe$	$C_{12}H_8N_8Ag_2Fe$	$C_{12}H_8N_8Ag_2Fe$
formula weight	535.85	535.85	535.85
crystal system	monoclinic	orthorhombic	orthorhombic
space group	*C*2/*c*	*Pccn*	*Pccn*
a (Å)	6.9750(3)	15.7700(2)	14.8950(2)
b (Å)	16.1700(9)	8.2980(4)	8.1580(4)
c (Å)	14.2020(8)	13.4180(6)	13.3480(5)
β (deg)	97.954(2)		
V (Å^3)	1586.37(14)	1755.87(12)	1621.96(10)
Z	4	4	4
D_c (mg cm^{-3})	2.244	2.027	2.194
F(000)	1024	1024	1024
μ(Mo Kα) (mm^{-1})	1.356	1.532	1.682
crystal size (mm^3)	0.03 × 0.05 × 0.06	0.04 × 0.06 × 0.07	0.04 × 0.06 × 0.07
temperature (K)	293(2)	250(2)	150(2)
no. of total reflections	1799	1993	1840
no. of reflections [$I > 2\sigma(I)$]	1291	1621	1572
R_1[a] [$I > 2\sigma(I)$]	0.0381	0.0251	0.0256
wR[a] [$I > 2\sigma(I)$]	0.0966	0.0582	0.0610
S	0.911	1.008	1.089

[a] $R_1 = \sum||F_o| - |F_c||/\sum|F_o|$; wR = $[\sum[w(F_o^2 - F_c^2)^2]/\sum[w(F_o^2)^2]]^{1/2}$; $w = 1/[\sigma^2(F_o^2) + (mP)^2 + nP]$ where $P = (F_o^2 + 2F_c^2)/3$; $m = 0.0723$ (**1**), 0.0289 (**2 HS**), and 0.0312 (**2 LS**); $n = 3.2523$ (**1**), 0.9112 (**2 HS**), and 0.3875 (**2 LS**).

full-matrix least squares analysis on F^2 using SHELXL-97.[14] All non-hydrogen atoms were refined anisotropically.

Differential Scanning Calorimetry (DSC). Calorimetric measurements have been performed on **2** using a differential scanning calorimeter (Mettler Toledo DSC 821^e). Low temperatures were obtained with an aluminum block which was attached to the sample holder, refrigerated with a flow of liquid nitrogen, and stabilized at a temperature of 110 K. The sample holder was kept in a drybox under a flow of dry nitrogen gas to avoid water condensation. The measurements were carried out using around 20 mg of a powdered sample sealed in aluminum pans with a mechanical crimp. Temperature and heat flow calibrations were made with standard samples of indium by using its melting (429.6 K, 28.45 J g^{-1}) transition. An overall accuracy of ±0.2 K in the temperature and ±2% in the heat capacity is estimated. The uncertainty increases for the determination of the anomalous enthalpy and entropy due to the subtraction of an unknown baseline.

Results

Crystal Structure of 1. Compound **1** crystallizes in the monoclinic *C*2/*c* space group. Crystal and refinement data can be found in Table 1. Relevant bond lengths and angles are given in Table 2. The crystal structure is constituted of an infinite stack of double layers made up of two identical, parallel, interlocked, two-dimensional coordination polymers {Fe(pmd)$_2$[Ag(CN)$_2$]$_2$}. The iron(II) ions are located at an inversion center defining a distorted octahedral [FeN$_6$] site (Figure 1a). The equatorial positions are occupied by four cyanide nitrogen atoms belonging to the [Ag(CN)$_2$]$^-$ anions, while two pmd ligands occupy the remaining axial positions. The equatorial Fe−N bond distances [Fe−N(2) = 2.171(5) Å and Fe−N(3) = 2.124(5) Å] are shorter than those corresponding to the axial positions [Fe−N(1) = 2.276(4) Å]. Each [Ag(CN)$_2$]$^-$ anion connects two Fe(II) atoms defining a two-dimensional grid (Figure 2a). The dimensions

Table 2. Selected Bond Lengths (Å) and Angles (deg) for **1** and **2**

	1	**2** (250 K)	**2** (150 K)
Fe−N(1)	2.276(4)	2.230(2)	2.002(2)
Fe−N(2)	2.171(5)	2.154(2)	1.946(2)
Fe−N(3)	2.124(5)	2.133(2)	1.932(2)
Ag−C(5)		2.078(3)	2.083(3)
Ag−C(6)		2.099(3)	2.107(3)
Ag1−C(6)	2.067(6)		
Ag2−C(5)	2.152(5)		
N(1)−Fe−N(2)	88.60(17)	87.31(8)	92.47(9)
N(1)−Fe−N(3)	89.91(17)	90.72(8)	89.14(9)
N(2)−Fe−N(3)	88.74(19)	90.05(9)	90.93(9)
C(5)−Ag−C(6)		161.54(12)	159.77(11)
C(5)−Ag−N(4)		102.17(10)	105.50(10)
C(6)−Ag−N(4)		93.21(10)	90.83(9)
C(6)−Ag1−C(6^i)[a]	176.7(3)		
C(5)−Ag(2)−C(5^i)[a]	138.8(3)		
C(5)−Ag(2)−N(4)	102.14(19)		

[a] $i = 1 - x, y, {}^1/_2 - z$.

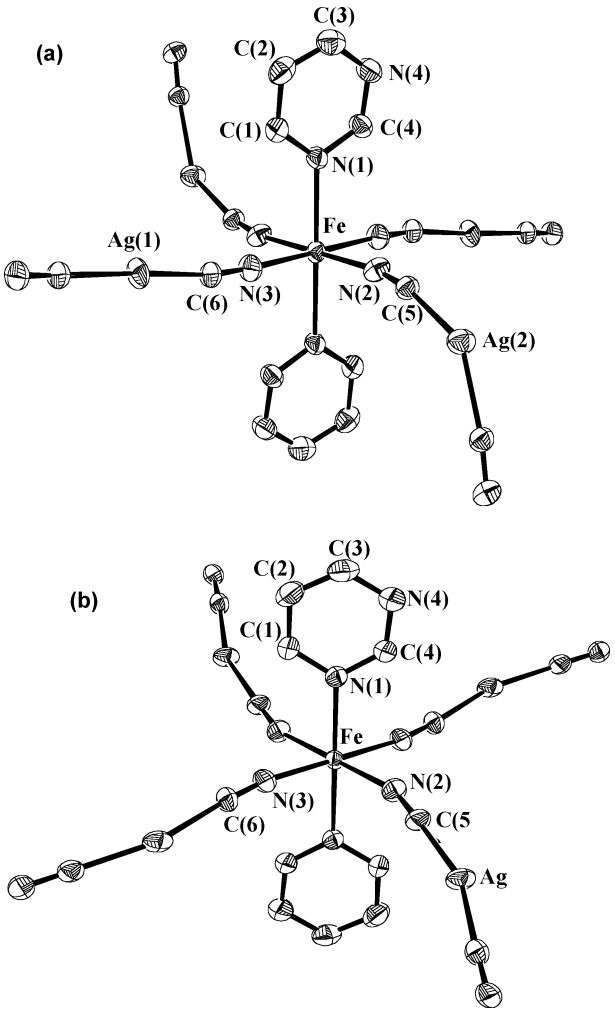

Figure 1. Perspective view of a representative fragment of **1** (a) and **2** (b) including the non-hydrogen atom numbering. Displacement ellipsoids are shown at the 50% probability level.

of the grids are 10.620 × 9.239 Å^2. There are two crystallographically distinct [Ag(CN)$_2$]$^-$ bridges referred as Ag(1) and Ag(2). Site Ag(1) is almost linear [C(6)−Ag(1)−C(6)^i = 176.7(3)°, $i = 1 - x, y, {}^1/_2 - z$], while site Ag(2) is strongly bent [C(5)−Ag(2)−C(5)^i = 138.8(3)°, $i = 1 - x, y, {}^1/_2 - z$]. The Ag−C bond distance is significantly shorter for site Ag(1) [Ag(1)−C(6) = 2.067(6) Å] than for site Ag-

(14) Sheldrick, G. M. *SHELXS97* and *SHELXL97*; University of Göttingen: Germany, 1997.

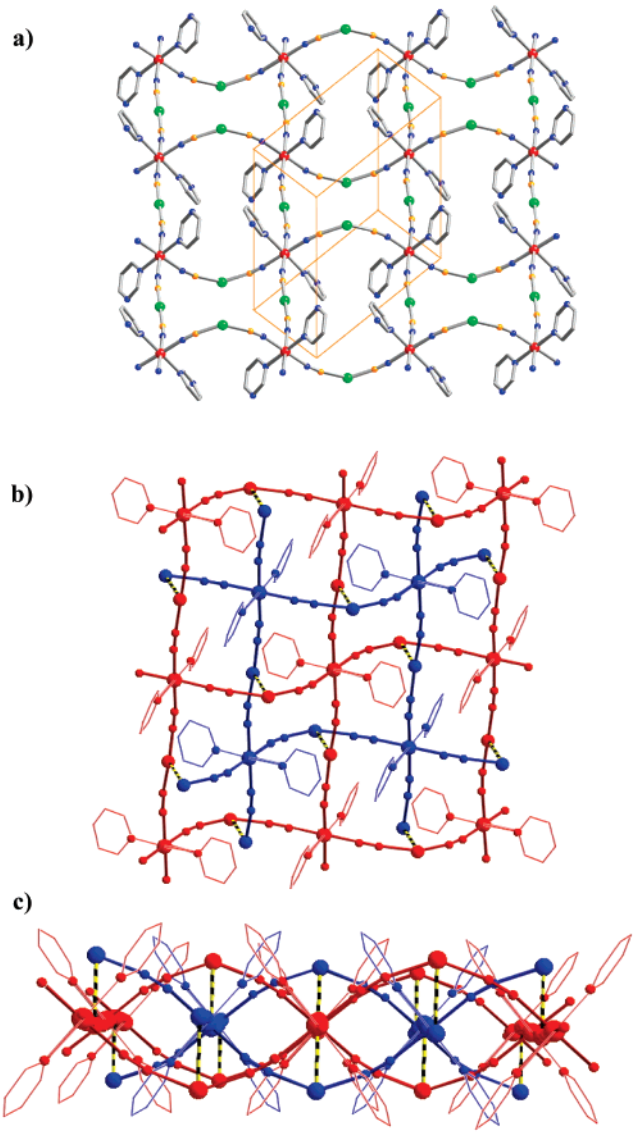

Figure 2. Structure of **1**: (a) view of a single layer showing the undulation of the {Fe(II)−[Ag(2)(CN)$_2$]$^-$−Fe(II)} chains; (b) view of two parallel interpenetrated layers; (c) view of the double layers in a perpendicular perspective. Dotted lines represent the strong argentophilic interactions observed in the double layers.

(2) [Ag(2)−C(5) = 2.152(5) Å]. However, the corresponding C−N lengths can be considered, within the error limits, to be identical [C(6)−N(3) = 1.147(8) Å and C(5)−N(2) = 1.142(7) Å for Ag(1) and Ag(2), respectively].

The grid is defined by two perpendicular systems of 1D {Fe[Ag(CN)$_2$]$_2$}$_\infty$ moieties where the iron atoms represent the corresponding knots. One moiety defined by site Ag(1) is an almost linear infinite chain, while the other, defined by site Ag(2), is an undulated infinite chain. Two consecutive undulated parallel {Fe[Ag(2)(CN)$_2$]$_2$}$_\infty$ chains are disposed as in phase and out of phase sinusoidal functions along the 2D layer (Figure 2a). This singular disposition defines a system of parallel channels, which are threaded by the linear {Fe[Ag(1)(CN)$_2$]$_2$}$_\infty$ moieties of the two interpenetrated layers. Strong argentophilic interactions occur between the interlocked layers. The Ag(1)····Ag(2) distance is 2.9972(10) Å (Figure 2b and c).

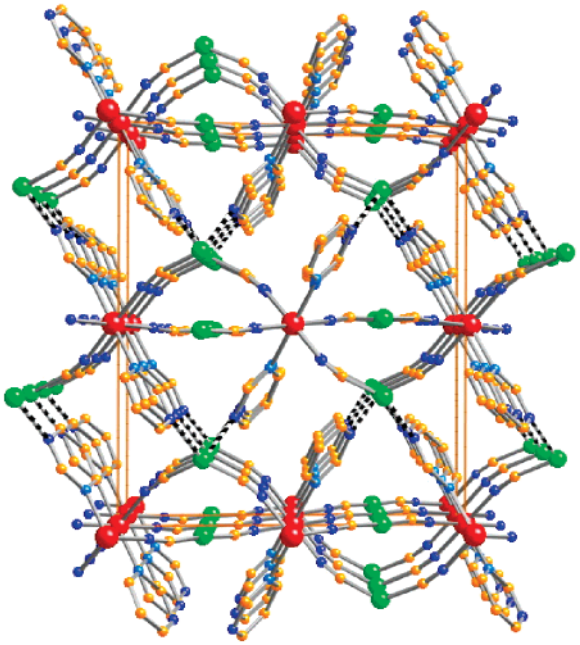

Figure 3. Crystal packing of the double layers in **1**. Dotted lines represent the coordinative interactions between pmd and [Ag(2)(CN)$_2$]$^-$.

The pmd ligands point out of the double layer in such a way that the N(4) nitrogen atoms interact with the Ag(2) atom. More precisely, two N(4) atoms belonging to the same double layer, but different grid, coordinate the Ag(2), conferring to it a pseudotetrahedral coordination environment (Figure 3). Apparently this interaction, Ag(2)−N(4) = 2.533(5) Å, is strong enough to provoke the remarkable distortion of the [Ag(2)(CN)$_2$]$^-$ anions mentioned above and to confer a 3D character to the coordination polymer.

Crystal Structure of 2. The crystal structure of **2** has been studied at 250 K and at 150 K. It displays the same orthorhombic *Pccn* space group at both temperatures. Crystal and refinement data can be found in Table 1. Relevant bond lengths and angles are given in Table 2. As in **1**, the iron(II) atom of **2** lies in an inversion center also having a similar coordination environment (Figure 1b). The axial positions, occupied by the pmd ligands [Fe−N(1) = 2.230(2) Å at 250 K and 2.002(2) Å at 150 K], are larger than the equatorial positions, occupied by the cyanide groups of the [Ag(CN)$_2$]$^-$ anions [Fe−N(2) = 2.154(2) Å and Fe−N(3) = 2.133(2) Å at 250 K and 1.946(2) Å and 1.932(2) Å at 150 K, respectively]. In contrast to the case of **1**, there is only one crystallographically independent [Ag(CN)$_2$]$^-$ anion in **2**. It is bent, as the angle C(5)−Ag−C(6) = 161.54(12)° at 250 K [159.77(11)° at 150 K] deviates 18.46° [20.23°] from linearity. The Ag−C bond distances are Ag−C(5) = 2.078(3) [2.083(3)] Å and Ag−C(6) = 2.099(3) [2.107(3)] Å, whereas the corresponding C−N distances are C(5)−N(2) = 1.142(3) [1.147(4)] Å and C(6)−N(3) = 1.133(4) [1.147(4)] Å. These structural parameters are similar to those observed previously for other iron(II)−dicyanoargentate systems.

As in the case of **1**, the [Ag(CN)$_2$]$^-$ anion bridges the defining layers of two iron atoms, which lie in the *a*,*b* plane and stack along the *b* axis. However, in this polymorph, no

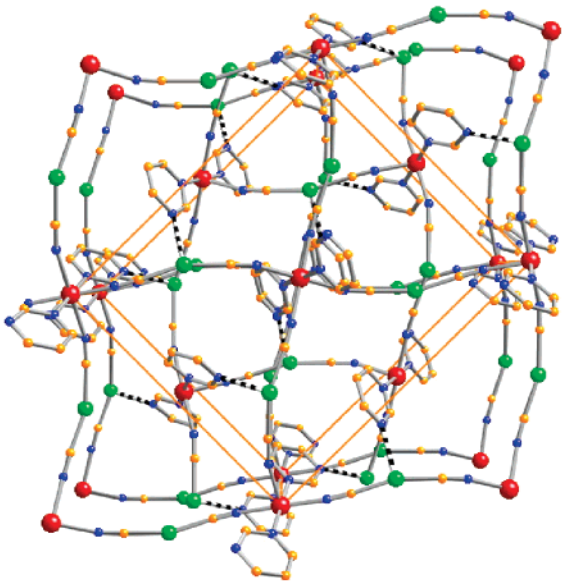

Figure 4. Crystal packing of the layers in **2**. Dotted lines represent the coordinative interactions between pmd and $[Ag(CN)_2]^-$.

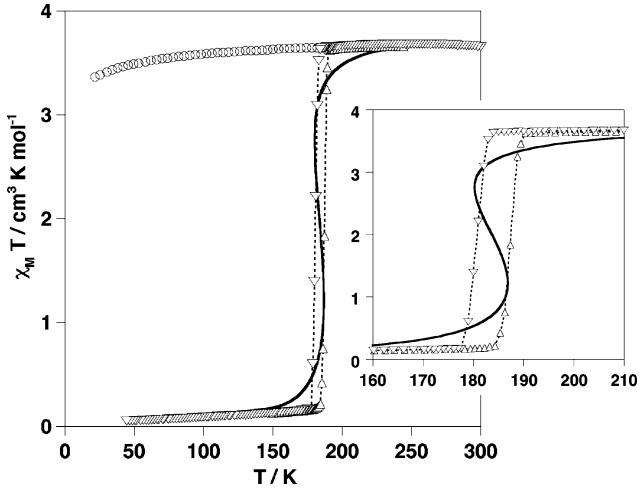

Figure 5. $\chi_M T$ versus T plot for **1** (○) and **2** (△). The inset represents a magnification of the hysteresis loop (▽ and △ represent the cooling and heating modes, respectively). The solid line corresponds to the best simulation of the experimental data (see text).

interpenetration occurs. Two consecutive layers are rotated by 45° with respect to each other, and the parallel layers are alternated so that the iron atoms of one layer lie vertically above and below the centers of the $\{Fe[Ag(CN)_2]\}_4$ rhombuses formed by the iron atoms of the adjacent layers. The peripheral N(4) atoms of the pmd groups of one layer point toward and coordinate the Ag atoms of the adjacent layers, conferring to these atoms a coordination number equal to 3. A similar situation has been described for other 3D coordination polymers (Figure 4). The Ag−N(4) distance 2.595(3) [2.574(2)] Å is a bit larger than that observed for **1**. However, the angular distortion of the $[Ag(CN)_2]^-$ anion in **2** denotes that the coordination of the N(4) is effective.

Magnetic Measurements. The thermal dependences of the product $\chi_M T$ for compounds **1** and **2** are displayed in Figure 5, χ_M being the molar magnetic susceptibility and T the temperature. For **1**, $\chi_M T$ is equal to 3.64 cm^3 K mol^{-1} at 196 K, which is in the range of the values expected for an

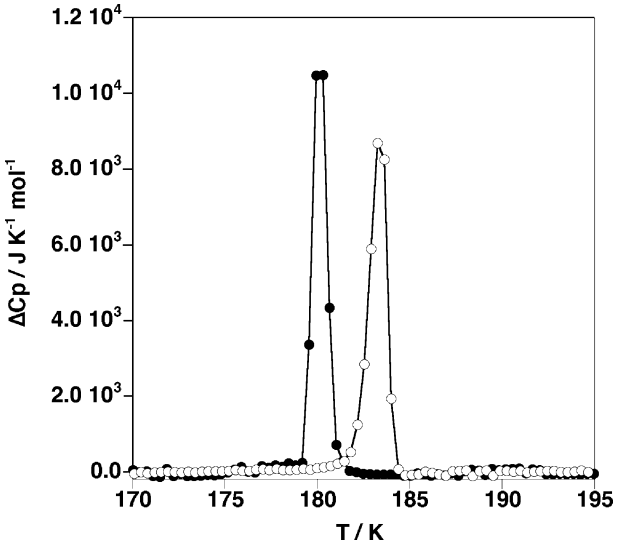

Figure 6. Thermal dependence of ΔC_p in the spin transition region. The ● and ○ symbols correspond to the cooling and heating modes, respectively.

iron(II) ion in the HS state. For lower temperatures, $\chi_M T$ decreases smoothly even at temperatures as low as 20 K, indicating that the $S = 2$ HS ground state does not split significantly at zero field. The $\chi_M T$ value is close to 3.68 cm^3 K mol^{-1} at room temperature for **2**. Upon cooling, $\chi_M T$ remains almost constant down to ca. 185 K, a temperature value after which it undergoes a very sharp decrease that is characteristic of a first-order SCO transition. The $\chi_M T$ value drops down to 0.13 cm^3 K mol^{-1} at 175 K. The warming mode reveals the occurrence of thermal hysteresis. The critical temperatures for the cooling (T_c^{down}) and warming (T_c^{up}) modes (181.1 and 186.3 K, respectively) indicate the occurrence of an ca. 5 K wide hysteresis loop. At temperatures below T_c, the $\chi_M T$ value indicates that virtually 100% of the iron(II) ions have converted into the LS state. This spin transition is accompanied by a drastic and reversible change of color from yellow (HS) to deep red (LS).

DSC Measurements for 2. The calorimetric measurements were carried out in the 150−220 K temperature range. A smooth line has been interpolated from the values in the normal regions, below 175 K and above 185 K. The heat capacity due to the transition has been deduced by subtraction of this baseline. The temperature dependence of the anomalous heat capacity, C_p, in the heating and cooling modes for **2** is shown in Figure 6. The temperatures of the maxima of the heat capacity curves were obtained for heating and cooling thermograms measured at different rates. The extrapolation at the zero-rate gave a transition temperature on heating and cooling of 183 and 180 K, respectively, indicating the occurrence of a hysteresis 3 K wide. These values agree reasonably well with those observed from the $\chi_M T$ vs T plot. The overall enthalpy (ΔH) and entropy (ΔS) variations associated with the spin transition determined from the DSC curves are $\Delta H = 11.5 \pm 0.4$ kJ mol^{-1} and $\Delta S = 64 \pm 3$ J K^{-1} mol^{-1} for the cooling mode and $\Delta H = 11.0 \pm 0.4$ kJ mol^{-1} and $\Delta S = 60 \pm 3$ J K^{-1} mol^{-1} for the warming mode.

Discussion

Self-assembly of $[Ag(CN)_2]^-$, pmd, and iron(II) has generated a rich variety of singular coordination polymeric networks, namely

$$\{Fe(pmd)_2[Ag(CN)_2]_2\} \quad (\mathbf{1})$$

$$\{Fe(pmd)_2[Ag(CN)_2]_2\} \quad (\mathbf{2})$$

$$\{Fe(pmd)(H_2O)[Ag(CN)_2]_2\}\cdot H_2O \quad (\mathbf{3})$$

$$\{Fe(pmd)[Ag(CN)_2]_2\} \quad (\mathbf{4})$$

$$\{Fe(pmd)[Ag_3(CN)_2][Ag(CN)_2]\} \quad (\mathbf{5})$$

which present interesting structural, physical, and chemical properties. A first question involving the chemical diversity of the Fe-pmd-$[Ag(CN)_2]$ system arises and concerns the synthesis of **1**−**5**. Except compound **4**, which was obtained from the dehydration of **3**, the remaining polymers were isolated as single crystals from the slow diffusion of water solutions in H-shaped vessels.[9c] Single crystals of **3** and **5** form exclusively when the temperature is kept close to 280 K during the diffusion process. Compound **3** appears rapidly (during the first week) as yellow polyhedral crystals while **5** crystallizes as well-defined clumps of flattened pale-yellow prismatic crystals in the subsequent 2−4 weeks.[9c,11] Single crystals of **1** and **2** grow in the diffusion vessel when the temperature is kept at around 303 K (small amounts of crystals of **3** were also separated in some experiments). They are easily separated using a binocular lens, as they have distinct colors, pale-yellow and orange-yellow for **1** and **2**, respectively. Polymorph **2** and compound **3** were also obtained by direct precipitation. However, in only a few cases, the samples consisted of **2** or **3** in pure phases, since usually they precipitate as a mixture of both. Because **2** and **3** display very different sharp spin transitions, it was easy to detect them and even to know their relative amounts in the mixture. Unfortunately, we did not succeed in separating the two components from the precipitated mixtures.

The five polymers have been characterized structurally. Let us briefly remember the structure of **3**−**5**. Compound **3** has two iron(II) sites interconnected by the $[Ag(CN)_2]^-$ groups, which occupy the equatorial positions of the irons. While one iron site has two terminal pmd ligands in the axial positions, the other iron site has two coordinated water molecules. Both sites alternate in defining a highly porous net with the $CdSO_4$ topology. In fact, three identical nets interpenetrate each other. Only the $[FeN_6]$ site (average Fe−N = 2.1649(19) Å) undergoes a cooperative spin transition centered at 219 K. In this polymer, the pmd ligands do not coordinate the silver atoms of the $[Ag(CN)_2]^-$ groups, which remain essentially linear. The uncoordinated nitrogen atoms of the pmd ligands in one net interact via hydrogen bonding with the coordinated water molecules of the adjacent nets in such a way that dehydration of the solid provokes the coalescence of the three independent nets into a new 3D net where the pmd ligands act as bridges between the iron atoms. The new net (compound **4**) undergoes a cooperative spin transition centered at around 133 K and transforms reversibly into **3** when it is exposed to water vapor. Compound **5** is rather singular in this series of compounds, as it contains the uncommon bridging ligand $[Ag_2(CN)_3]^-$ which forms in situ during the crystallization process. It defines a very complicated self-interpenetrated 3D network displaying a thermal and light induced two-step spin transition with $T_{c1} = 146.7$ K and $T_{c2} = 185$ K.

Compounds **1** and **2** have the same chemical formula but display different crystal structures. From this point of view, they can be considered polymorphs. It is also important to stress that both polymorphs crystallize under identical physical conditions in the same H-shaped vessel. These compounds can be viewed as 3D coordination polymers made up of a stack of a series of layers constituted of $[Ag(CN)_2]^-$ and iron(II) atoms defining square $\{Fe_4[Ag(CN)_2]_4\}_n$ grids. The pmd groups, which lie in the iron(II) axial positions, interact with the silver atoms belonging to the adjacent layers, defining the 3D architectures. The architectural isomerism represented by **1** and **2** is associated with the conformational changes occurring in the usually rigid $[Ag(CN)_2]^-$ ligands. More precisely, the $[Ag(2)(CN)_2]^-$ anion has an uncommon distorted bent geometry [C(5)−Ag(2)−C(5) = 138.8(3)°] in compound **1**, which induces strong undulation of the $\{Fe[Ag(2)(CN)_2]_2\}_\infty$ chains and allows parallel interpenetration of two identical layers. This strong deviation from linearity is a consequence of the coordination of two peripheral nitrogen atoms of two pmd ligands belonging to a contiguous layer, which confers to the Ag(2) atom a distorted tetrahedral geometry. In the case of polymorph **2**, the $[Ag(CN)_2]^-$ ligand is remarkably less bent [C(5)−Ag−C(6) = 161.8(3)°] and the $\{Fe[Ag(CN)_2]_2\}_\infty$ chains are only slightly corrugated; consequently, no interpenetration occurs. Connectivity takes place between adjacent layers through coordination of the Ag atoms by the peripheral nitrogen atoms of the pmd ligands in **2**. The average Fe−N bond distance is $R = 2.190$ and 2.172 Å for **1** and **2**, respectively. Taking into account the fact that the ligand field strength, Δ_o, is proportional to $1/R^6$, an increase of ca. 4.8% is estimated when moving from **1** to **2**. As observed in the preceding examples, this increase in Δ_o is enough to induce a thermal spin transition in **2** at ambient pressure. Pressure usually causes a tendency toward a closer packing of molecules, and consequently, it intensifies the intermolecular interactions and makes the metal-to-ligand bond distances shorter, enhancing the ligand field strength.[15] For instance, the paramagnetic mononuclear polymorph B of the system $[Fe(abpt)_2(NCS)_2]$ (abpt = 4-amino-3,5-bis(pyridin-2-yl)-1,2,4-triazole) displays an average Fe−N bond distance 0.023(5) Å greater than that of the SCO polymorph A (T_c = 180 K), which represents a difference of ca. 6% in terms of Δ_o.[16] The application of pressure to polymorph B enables

(15) (a) Drickamer, H. G. *Solid State Phys.* **1965**, *17*, 1. (b) Stephens, D. R.; Drickamer, H. G. *J. Phys. Chem.* **1982**, *2*, 171.

(16) Moliner, N.; Muñoz, M. C.; Létard, S.; Létard, J. F.; Solans, X.; Burriel, R.; Castro, M.; Kahn, O.; Real, J. A. *Inorg. Chim. Acta* **1999**, *291*, 279.

the observation of thermal induced SCO. In particular, at ca. 0.9 GPa polymorph B undergoes a SCO essentially identical to that observed for polymorph A at 10^5 Pa.[17] As far as compounds **1** and **2** are concerned, it is reasonable to expect that the application of pressure to **1** could induce a thermal SCO similar to that observed for **2**. However, despite the small difference observed in Δ_o for **1** and **2**, the former does not undergo a thermal spin transition even at 0.9 GPa. Given that we do not know the crystal structure of **1** under pressure, it is difficult to associate this behavior with the singular disposition of the interlocked double layers and the interplay between them via strong argentophilic interactions.

It is instructive to compare the structure of **2** with that of $\{Fe(pyrazine)[Ag(CN)_2]_2\}\cdot$pyrazine. This latter compound also forms an infinite stack of parallel 2D arrays defined by $\{Fe_4[Ag(CN)_2]_4\}$ units. However, the coordination topology of the pyrazine ligand allows pillaring of these layers through the connection of the Fe(II) ions belonging to the adjacent layers. The 1 and 3 positions of the donor nitrogen atoms in pmd determine the different arrangement of the layers in **2**. So, the pmd groups in one layer point toward the center of the windows defined by the $\{Fe_4[Ag(CN)_2]_4\}$ units. This fact favors the coordination of the N(4) atoms to the Ag(I) ions in **2**. It is worth mentioning that at room temperature the iron(II) ions in the pyrazine derivative are LS, while they are HS in **2**.

Consistency between the magnetic and thermodynamic data has been checked using the expression (eq 1) derived from the regular solution model,[18]

$$\ln[(1-\gamma_{HS})/(\gamma_{HS}-f_{HS})] = [\Delta H + \Gamma(f_{HS}+1-2\gamma_{HS})]/RT - \Delta S/R \quad (1)$$

where ΔH and ΔS represent the average values obtained from the cooling and warming modes and Γ is the parameter accounting for the cooperativity associated with the spin conversion. The HS molar fraction, γ_{HS}, has been defined as follows (eq 2),

$$\gamma_{HS} \approx (\chi_M T)_T/(\chi_M T)_{HS} \quad (2)$$

where $(\chi_M T)_T$ is the value of $\chi_M T$ at any temperature and $(\chi_M T)_{HS}$ corresponds to the pure HS state. The parameter f_{HS} accounts for the HS molar fraction at low temperature (eq 3),

$$f_{HS} \approx (\chi_M T)_{LT}/(\chi_M T)_{HS} \quad (3)$$

where $(\chi_M T)_{LT}$ corresponds to the value of $\chi_M T$ at low temperature once the spin conversion is accomplished. In the present case, $(\chi_M T)_{LT}$ is close to 0.13 cm^3 K mol^{-1}, a value that corresponds to $f_{HS} \approx 0.035$. Least-squares fitting leads to $\Gamma = 3.9$ kJ mol^{-1}, $\Delta H \approx 11.27$ kJ mol^{-1}, $\Delta S = 61.25$ J K^{-1} mol^{-1}, and $(\chi_M T)_{HS} = 3.76$ cm^3 K mol^{-1} (solid line in Figure 5). These ΔH and ΔS values correspond quite well to those deduced from the calorimetric measurements. The Γ value deduced from the fit is greater than $2RT_c$ ($T_c = 184$ K), a necessary condition which ensures the occurrence of hysteresis.[19] To obtain a realistic fit, $(\chi_M T)_{HS}$ was considered to be an adjustable parameter. The obtained $(\chi_M T)_{HS}$ value is slightly larger than the maximum value, $\chi_M T = 3.68$ cm^3 K mol^{-1}, deduced experimentally. This situation is not uncommon in SCO compounds. For instance, the mononuclear system $\{Fe[H_2B(pz)_2]_2L\}$ where $[H_2B(pz)_2]^-$ is the anion dihydrobis(pyrazolyl)borate and L = phenanthroline (phen) or 2,2′-bipyridine (bipy)[20] undergoes apparently complete LS-to-HS transitions at $T > T_c$; however, the experimental thermodynamic parameters obtained from calorimetric measurements where not consistent with the Mössbauer experiments which indicated the occurrence of 8% and 15% LS species at $T > T_c$ for bipy and phen derivatives, respectively.[20b] In the present case, apparently ca. 2.5% of the centers remain LS at $T > T_c$, a value which is required to obtain a correct simulation of the experimental data. As expected, the ΔS value for **2** is significantly larger than the entropy variation resulting from the change in spin-only values ($\Delta S = R \ln[(2S_{HS}+1)/(2S_{LS}+1)] = 13.4$ J mol^{-1} K^{-1} for $S_{HS} = 2$ and $S_{LS} = 0$). The excess of entropy, ca. 48 J mol^{-1} K^{-1}, mainly corresponds to the structural changes associated with the [Fe−N_6] bond lengths observed, which are on average 0.212(2) Å shorter in the LS state for **2**. The longer bond lengths of the HS state decrease the interatomic force constants, reducing the corresponding vibrational frequencies. As a result, the number of excited vibrational states experiences an abrupt jump with the lattice expansion and, consequently, the entropy increases with the LS-to-HS transition temperature.

Acknowledgment. Financial support is acknowledged from the Spanish Ministerio de Educacion y Ciencia (MEC) (CTQ 2004-03456/BQU). A.G. thanks the Universitat Politécnica de València for a predoctoral fellowship. A.B.G. thanks the Spanish MEC for a research contract (Programa Ramón y Cajal).

Supporting Information Available: CIF data. This information is available free of charge via the Internet at http://pubs.acs.org.

IC0509074

(17) Gaspar, A. B.; Muñoz, M. C.; Moliner, N.; Ksenofontov, V.; Levchenko, G.; Gütlich, P.; Real, J. A. *Monatsh. Chem.* **2003**, *134*, 285.
(18) Slichter, C. P.; Drickamer, H. G. *J. Chem. Phys.* **1972**, *56*, 2142.
(19) Honig, J. M. *J. Chem. Educ.* **1999**, *76*, 848.
(20) (a) Real, J. A.; Muñoz, M. C.; Faus, J.; Solans, X. *Inorg. Chem.* **1997**, *36*, 3008. (b) Moliner, N.; Salmon, L.; Capes, L.; Muñoz, M. C.; Létard, J. F.; Bouseksou, A.; Tuchagues, J. P.; McGarvey, J. J.; Dennis, A. C.; Castro, M.; Burriel, R.; Real, J. A. *J. Phys. Chem. B* **2002**, *106*, 4276. (c) Thompson, A. L.; Goeta, A. E.; Real, J. A.; Galet, A.; Muñoz, M. C. *Chem. Commun.* **2004**, 1390.